Ersin Demir, Hasan Çallioğlu* and Metin Sayer

Vibration analysis of sandwich beams with variable cross section on variable Winkler elastic foundation

Abstract: In this study, free vibration behavior of a multilayered symmetric sandwich beam made of functionally graded materials (FGMs) with variable cross section resting on variable Winkler elastic foundation are investigated. The elasticity and density of the functionally graded (FG) sandwich beam vary through the thickness according to the power law. This law is related to mixture rules and laminate theory. In order to provide this, a 50-layered beam is considered. Each layer is isotropic and homogeneous, although the volume fractions of the constituents of each layer are different. Furthermore, the width of the beam varies exponentially along the length of the beam, and also the beam is resting on an elastic foundation whose coefficient is variable along the length of the beam. The natural frequencies are computed for conventional boundary conditions of the FG sandwich beam using a theoretical procedure. The effects of material, geometric, elastic foundation indexes and slenderness ratio on natural frequencies and mode shapes of the beam are also computed and discussed. Finally, the results obtained are compared with a finite-element-based commercial program, ANSYS®, and found to be consistent with each other.

Keywords: elastic foundation; free vibration; functionally graded materials; variable cross section.

***Corresponding author: Hasan Çallioğlu,** Department of Mechanical Engineering, Pamukkale University, Kinikli Campus, 20070 Denizli, Turkey, e-mail: hcallioglu@pau.edu.tr
Ersin Demir and Metin Sayer: Department of Mechatronics Engineering, Pamukkale University, Kinikli Campus, 20070 Denizli, Turkey

1 Introduction

Functionally graded materials (FGMs) are obtained by changing the volume fractions of constituents from one surface to the other gradually. Thus, the material properties of the structure can be adjusted according to demand. Because of this advantage, these materials have attracted the attention of many researchers [1–4]. The field has been developed rapidly because of their wide practical application in machine, civil, aerospace and automotive areas. Among these areas, dynamic analysis of beams made of FGMs has been studied by some researchers. Aydogdu and Taskin [5] investigated free vibration of simply supported FG beam by using parabolic, first-order and exponential shear deformation beam theories. Aydogdu [6] used the semi-inverse method to find a relation between elasticity modulus and natural frequency and buckling. Pradhan and Murmu [7] presented thermomechanical vibration analysis of beams and sandwich beams made of FGM under different conditions. Bedjilili et al. [8] coped with the free vibration of composite beams with a variable fiber volume fraction using the first-order shear deformation theory. A fourth-order differential equation of a homogenized beam deflection was dealt with by Murin et al. [9]. Mahi et al. [10] analyzed the free vibration of a symmetric FG beam subjected to initial thermal stresses by using a theoretical formulation, and they assumed the material properties as temperature dependent.

Additionally, there are some studies related to free vibration behavior of beams with variable cross section. Ece et al. [11] investigated the vibration of an isotropic beam, which has variable cross section. Atmane et al. [12] presented a theoretical investigation for free vibration of an FG beam with variable cross section. Their theory was based on the Kirchhoff-Love hypothesis and they only changed the material properties as exponential. Cranch and Adler [13] presented the closed-form solution for the natural frequencies and mode shapes of unconstrained nonuniform beams with four kinds of rectangular cross sections. Caruntu [14] examined the nonlinear vibrations of beams with rectangular cross section and parabolic thickness variation. Datta and Sil [15] determined numerically the natural frequencies of cantilever beams with constant width and linearly varying depth. Laura et al. [16] used approximate numerical approaches to determine the natural frequencies of Bernoulli beams with constant width and bilinearly varying thickness.

In other words, beams resting on elastic foundations have wide application in engineering practice. As a result, some researches have been performed to investigate the dynamic response of the beams resting on various elastic foundations, such as the Winkler, Pasternak and Vlasov models. Some of these are given as follows.

Ayvaz and Özgan [17] applied a modified Vlasov model to free vibration analysis of beams resting on elastic foundations, and they analyzed the effects of the subsoil depth, the beam length, their ratio and the value of the vertical deformation parameter within the subsoil on the frequency parameters of beams on elastic foundations. Motaghian et al. [18] solved the free vibration problem of beams on elastic foundation of the Winkler type, which is distributed over a particular length of the beam. They proposed an innovative mathematical approach to find a precise analytical solution of the free vibration of beams. Ying et al. [19] presented exact solutions for bending and free vibration of FG beams resting on a Winkler-Pasternak elastic foundation based on the two-dimensional theory of elasticity. They solved the problem by using the state space method.

Natural frequencies obtained from the aforementioned studies are generally about isotropic beams either with variable cross sections or on elastic foundation, or FG beams with constant cross section. Some studies on FG beams with variable cross sections are solved via plate hypotheses. The difference of this study from the others is that the Euler-Bernoulli beam hypothesis is modified for natural frequencies of sandwich laminated FG beams. Therefore, this study shows that the effective elasticity modulus and the effective mass density can be used instead of elasticity modulus and mass density in the governing differential equation of motion for a beam made of conventional materials in this hypothesis.

In this work, free vibration behavior of a symmetric FG sandwich beam with variable cross section on the variable elastic foundation is analyzed. The material properties (effective elasticity modulus and mass density) of the FG sandwich beam vary through the thickness according to the power law, whereas the width of the beam with rectangular cross section changes exponentially along the length of the FG beam. Natural frequencies are found by using obtained effective material properties for various boundary conditions. The results obtained are compared with ANSYS® solutions, and all results are found to be consistent with each other. The effects of material, geometrical and elastic foundation indexes and slenderness ratio on the vibration behavior of the sandwich beam with variable cross section are also discussed.

2 Determination of the effective material and geometry properties

Consider a transversely vibrating symmetric sandwich beam with variable cross section made of FGM on a

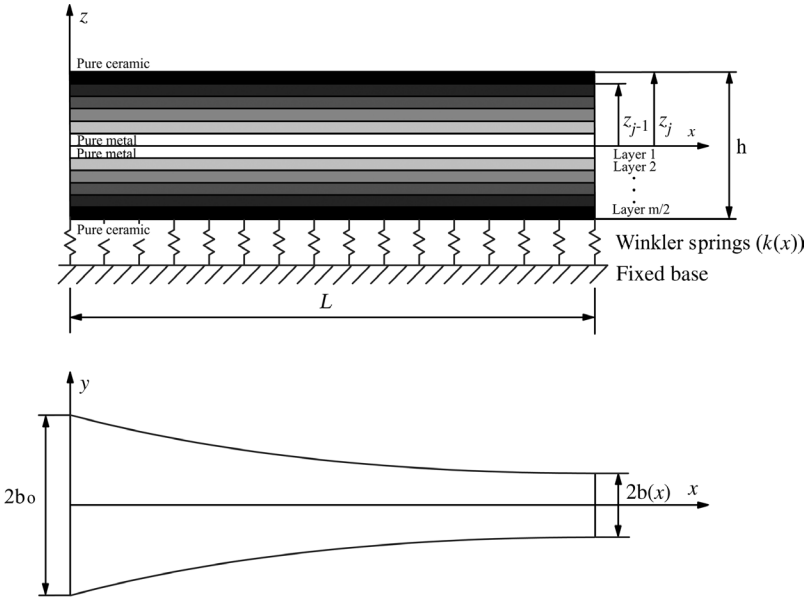

Figure 1 An FG sandwich beam with variable cross section on variable Winkler foundation.

variable Winkler elastic foundation as shown in Figure 1. Here; L and h represent the length and thickness of the beam, respectively. b_0 is the half-width at the left end of the beam. However, the width of the beam $b(x)$ is supposed to vary exponentially along the length of the beam as follows,

$$b(x)=b_0\, e^{\beta x} \tag{1}$$

where β is the geometric index, and as β=0 the beam has uniform cross section.

The beam is assumed to be composed of 50 FG layers in order to get a more consistent value in the solution. Each layer is a mixture of aluminum (Al) and alumina (Al_2O_3) phases, and layers are arranged symmetrically to the neutral plane of the beam. That is, the beam is stacked as $[Al_2O_3/FGM/Al]_s$. The mixture ratio is chosen as a polynomial function, and it varies continuously and symmetrically through the thickness with respect to the neutral plane of the beam.

In order to obtain the effective material properties of the whole structure, the following procedure is applied. First, the material properties of the upper half of the beam are calculated from the power law as given in Eqs. (2) and (3). Second, effective material properties of the whole structure are obtained by using the formula of effective elasticity modulus for symmetric laminated composite structures. The power law for elasticity modulus is given as follows:

$$E(z)=\left(E_c\text{-}E_m\right)\left(z+\frac{1}{2}\right)^n+E_m \tag{2}$$

where E_c, E_m, z and n are the elasticity moduli of ceramic and metal phases and the coordinate axis in the thickness direction of the beam and material index, respectively. The variation of mass density in each layer through the beam thickness has also been considered to obtain more accurate results. The expressions written for elasticity moduli are also considered to be valid for density.

$$\rho(z)=\left(\rho_c\text{-}\rho_m\right)\left(z+\frac{1}{2}\right)^n+\rho_m \tag{3}$$

The above-mentioned variable z is defined as $z=\text{-}\frac{1}{2},\text{-}\frac{1}{2}+\frac{1}{\eta},\text{-}\frac{1}{2}+\frac{2}{\eta},\cdots,\frac{1}{2}$, where η is equal to (m/2)-1, where m represents the number of the layer of the beam (see Figure 1).

It is seen from Figure 1 that the top and bottom surfaces of the FG beam are pure ceramic, whereas the middle section of the beam is pure metal. The variations of elasticity modulus and the mass density through the whole thickness of the beam for various material indexes (n) are shown in Figure 2A and B, respectively.

Eqs. (2) and (3) give the elasticity modulus and mass density for each layer in the upper half part of the beam, respectively. In order to find the elasticity modulus and the mass density throughout the whole beam thickness, the classical laminate theory will be used.

The bending moment on a symmetric FG sandwich beam can be written in a way similar to that used in laminated composite beam theory [20],

$$M=\frac{2b}{3r}\sum_{j=1}^{m/2}\left(E_z\right)_j\left(z_j^3\text{-}z_{j\text{-}1}^3\right) \tag{4}$$

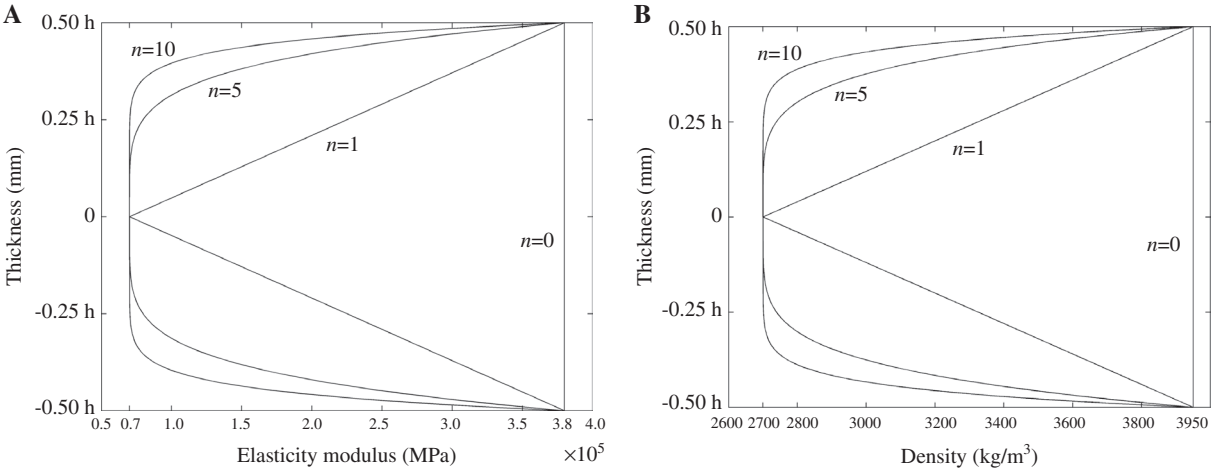

Figure 2 Variations of elasticity modulus (A) and mass density (B) through the thickness for different index values of power law functions.

where r and z_j are the curvature of the beam and the distance between the outer face of the jth layer and the neutral plane, respectively. The bending moment can also be written as follows:

$$M=\frac{E_{\text{ef}}I_{yy}}{r} \tag{5}$$

where E_{ef} is the effective elasticity modulus and I_{yy} is the cross-sectional inertia moment about the neutral axis of the beam. Substituting Eq. (4) into Eq. (5), the effective elasticity modulus can be written as

$$E_{\text{ef}}=\frac{8}{h^3}\sum_{i=1}^{m/2}\left(E_z\right)_j\left(z_j^3-z_{j-1}^3\right) \tag{6}$$

Similarly, the effective mass density can be written as follows,

$$\rho_{\text{ef}}=\frac{8}{h^3}\sum_{j=1}^{m/2}\left(\rho_z\right)_j\left(z_j^3-z_{j-1}^3\right) \tag{7}$$

In the calculation of the natural frequency, the effective elasticity modulus E_{ef} and the effective mass density ρ_{ef} can be used instead of elasticity modulus E and mass density ρ in a beam manufactured from isotropic and homogenous materials.

3 Theoretical formulation and solution

The governing differential equation of motion for a beam with variable cross section made of FGMs on a variable Winkler elastic foundation can be expressed as follows:

$$\frac{\partial^2 M}{\partial x^2}+\rho_{\text{ef}}A(x)\frac{\partial^2 w(x,t)}{\partial t^2}+k(x)w(x,t)=0,\qquad 0\le x\le L \tag{8}$$

and

$$M=E_{\text{ef}}I(x)\frac{\partial^2 w(x,t)}{\partial x^2} \tag{9}$$

where t is time, $A(x)=b(x)h$ is the variable cross-sectional area, $I(x)=b(x)\ h^3/12$ is the variable inertia moment, $k(x)=k_s b(x)$ is the variable foundation modulus and k_s is the elastic foundation index.

Putting Eq. (9) into Eq. (8) yields

$$\begin{aligned}&E_{\text{ef}}I(x)\frac{\partial^4 w(x,t)}{\partial x^4}+2E_{\text{ef}}\frac{dI(x)}{dx}\frac{\partial^3 w(x,t)}{\partial x^3}\\&+E_{\text{ef}}\frac{d^2I(x)}{dx^2}\frac{\partial^2 w(x,t)}{\partial x^2}+k(x)w(x,t)+\\&\rho_{\text{ef}}A(x)\frac{\partial^2 w(x,t)}{\partial t^2}=0\end{aligned} \tag{10}$$

The transverse displacement $w(x,t)$ can be expressed as

$$w(x,t)=W(x)e^{\omega t} \tag{11}$$

Similarly, putting Equation (11) into Equation (10) gives,

$$\begin{aligned}&E_{\text{ef}}I(x)\frac{d^4W(x)}{dx^4}+2E_{\text{ef}}\frac{dI(x)}{dx}\frac{d^3W(x)}{dx^3}\\&+E_{\text{ef}}\frac{d^2I(x)}{dx^2}\frac{d^2W(x)}{dx^2}+k(x)W(x)-\rho_{\text{ef}}A(x)W(x)\omega^2=0\end{aligned} \tag{12}$$

Substituting $A(x)$, $I(x)$ and $k(x)$ into Eq. (12) yields

$$\begin{aligned}&\frac{d^4W(x)}{dx^4}+2\beta\frac{d^3W(x)}{dx^3}+\beta^2\frac{d^2W(x)}{dx^2}\\&+\frac{12}{Eh^3}\left(k_s-\rho_{\text{ef}}h\omega^2\right)W(x)=0\end{aligned} \tag{13}$$

As Eq. (13) is solved, the following expression can be obtained,

$$W(x)=e^{-\frac{\beta}{2}x}\left(C_1e^{i\lambda_1 x}+C_2e^{-i\lambda_1 x}+C_3e^{\lambda_2 x}+C_4e^{-\lambda_2 x}\right) \tag{14}$$

Here, $\lambda_1=\sqrt{\mu-\beta^2h^4E^2}\,/\,2h^2E$ and $\lambda_2=\sqrt{\mu+\beta^2h^4E^2}\,/\,2h^2E$, where μ is equal to $8h^2E\sqrt{3}\sqrt{Eh\left(-k_s+\rho h\omega^2\right)}$ and C_1, C_2, C_3 and C_4 are (complex) constants. In other words, the solution can also be written in trigonometric form:

$$\begin{aligned}W(x)=e^{-\frac{\beta}{2}x}&\left(B_1\cos\left(\lambda_1 x\right)+B_2\sin\left(\lambda_1 x\right)+B_3\cosh\left(\lambda_2 x\right)\right.\\&\left.+B_4\sinh\left(\lambda_2 x\right)\right)\end{aligned} \tag{15}$$

where B_1, B_2, B_3 and B_4 are real constants and are determined by the boundary conditions.

Three different types of boundary conditions are considered in this study: clamped (C), simply supported (S) and free (F). These boundary condition types are described as,

$$\text{C}\rightarrow W=0;\ dW/dx=0 \tag{16}$$

$$\text{S}\rightarrow W=0;\ d^2W/dX^2=0 \tag{17}$$

$$\text{F}\rightarrow d^2W/dX^2=0;\ d^3W/dX^3=0 \tag{18}$$

The widely used boundary conditions are taken into account at two ends of the beam, i.e., C-C, C-S, S-S and C-F.

When the boundary conditions are applied to Eq. (15), four equations emerged from each boundary condition. The roots of these four equations are obtained from the determinant, which is composed of four equations. As a result of this, the characteristic equations can be found for each related boundary conditions.

For example, the following four equations are obtained by substitution of boundary conditions of CC into Eq. (15).

$$W(x)|_{x=0}=B_1+B_3=0 \tag{19a}$$

$$\left.\frac{dW(x)}{dx}\right|_{x=0}=-\frac{\beta B_1}{2}-\frac{\beta B_3}{2}+B_2\lambda_1+B_4\lambda_2=0 \tag{19b}$$

$$W(x)|_{x=L}=e^{\frac{\beta L}{2}}\left(B_1\cos(\lambda_1 L)+B_2\sin(\lambda_1 L)+B_3\cosh(\lambda_2 L)+B_4\sinh(\lambda_2 L)\right)=0 \tag{19c}$$

$$\begin{aligned}\left.\frac{dW(x)}{dx}\right|_{x=L}=&-\frac{1}{2}e^{\frac{\beta L}{2}}\left(\beta B_1\cos(\lambda_1 L)+\beta B_2\sin(\lambda_1 L)\right.\\&+\beta B_3\cosh(\lambda_2 L)+\beta B_4\sinh(\lambda_2 L)\\&+2\lambda_1 B_1\sin(\lambda_1 L)-2\lambda_1 B_2\cos(\lambda_1 L)\\&\left.-2\lambda_2 B_3\sinh(\lambda_2 L)-2\lambda_2 B_4\cosh(\lambda_2 L)\right)=0\end{aligned} \tag{19d}$$

The following characteristic equation is written by the determinant of matrix, which is obtained from Eq. (19):

$$\begin{aligned}&\left(e^{\frac{\beta L}{2}}\right)^2\left(\lambda_1\cosh(\lambda_2 L)^2\lambda_2-\lambda_1\sinh(\lambda_2 L)^2\lambda_2+\right.\\&\sin(\lambda_1 L)\lambda_2^2\sinh(\lambda_2 L)-2\cos(\lambda_1 L)\lambda_1\cosh(\lambda_2 L)\lambda_2\\&+\cos(\lambda_1 L)^2\lambda_2\lambda_1-\sin(\lambda_1 L)\lambda_1^2\sinh(\lambda_2 L)\\&\left.+\sin(\lambda_1 L)^2\lambda_1\lambda_2\right)=0\end{aligned} \tag{20}$$

In order to calculate the natural frequencies, these characteristic equations are solved numerically.

4 Results and discussion

In this study, the 50-layered FG sandwich beam with variable cross section on Winkler foundation is considered. The material properties of the constituents of the beam are given in Table 1. The elasticity modulus and density of the FG beam are chosen to be variable, whereas Poisson's ratio υ is considered as a constant. The thickness and length of the beam are constant and are set to h=5 mm and L=200 mm, respectively. The width is b_0=20 mm at the left end of the FG beam and changes exponentially along the length of the beam. Material index (n) is considered to be between 0 and 10, and geometric index (β) is taken from -1/L to 1/L with an interval of 0.25/L. The FG beam is isotropic, homogenous and uniform as n and β are equal to zero.

Table 1 Material properties of the constituents of the FG sandwich beam.

Material	E (GPa)	ρ (kg/m³)	υ
Al	70	2700	0.3
Al_2O_3	380	3950	0.3

The variable elastic foundation is designed on the basis of Winkler modeling. The variable foundation modulus $k(x)$ varies according to elastic foundation index k_s through the length of the beam as mentioned above. In this study, k_s is taken to be from 0 to 1000.

In order to support the accuracy of the results obtained from the present method, the beam is also solved by the commercial program ANSYS® using finite element analyses. The beam is modeled and meshed by SHELL 63 which has six degrees of freedom at each node. The elastic foundation stiffness (EFS) can be added to the beam model in this element type. This element is quite well suited for computing natural frequencies of beams that have EFS. The beams with variable cross section are modeled by SOLIDWORKS® program and imported to ANSYS as IGS files. In mesh refinement, an element is utilized per square millimeter of the cross section. In the solution, 6868 elements and 7100 nodes are utilized for the C-C beam with β=1/L. The block Lanczos method is used for the eigenvalue extractions to calculate frequencies.

Table 2 and Figures 3–5 represent the variations of the natural frequencies for mode 1 of the FG cantilever beam, which are obtained with both present and ANSYS solutions, versus material index (n), geometrical index (β) and elastic foundation index (k_s). Moreover, Table 2 shows the error rate (%) between present and ANSYS results.

4.1 Effect of material index

Figure 3 illustrates the variations of the natural frequencies of an FG beam with β=-1/L and k_s=100 versus material

Table 2 Comparison of the results of the present and ANSYS for CF boundary condition.

	β=-1/L, k_s=100				β=-1/L, n=1				n=1, k_s=100		
n	Present	ANSYS	Error (%)	k_s	Present	ANSYS	Error (%)	β	Present	ANSYS	Error (%)
0	11328.1	11328.3	0.0017	0	248.8	250.1	0.5210	-1/L	11783.8	11784.0	0.0017
1	11783.8	11784.0	0.0017	100	11783.8	11784.0	0.0017	-0.75/L	11783.4	11783.6	0.0017
2	12080.4	12080.6	0.0013	200	16663.0	16663.2	0.0013	-0.5/L	11783.1	11783.3	0.0018
3	12289.2	12289.4	0.0016	300	20407.1	20407.4	0.0016	-0.25/L	11782.9	11783.0	0.0008
4	12444.2	12444.5	0.0020	400	23563.7	23564.0	0.0013	0	11782.6	11782.8	0.0015
5	12563.9	12564.1	0.0015	500	26344.7	26345.1,	0.0014	0.25/L	11782.4	11782.6	0.0012
6	12659.0	12659.2	0.0013	600	28859.0	28859.4	0.0012	0.5/L	11782.2	11782.4	0.0014
7	12736.3	12736.5	0.0015	700	31171.1	31171.5	0.0012	0.75/L	11782.1	11782.2	0.0008
8	12800.3	12800.6	0.0020	800	33323.1	33323.6	0.0014	1/L	11781.9	11782.1	0.0013
9	12854.3	12854.5	0.0013	900	35344.4	35344.9	0.0013				
10	12900.2	12900.4	0.0017	1000	37256.2	37256.7	0.0013				

index (n) for C-F (cantilever) boundary conditions. It can be seen from the figure that natural frequencies increase with increasing material index (n). Namely, an increase in the volume fractions of the ceramic phase in the FG sandwich beam causes a decrease in the natural frequencies. As a result, in order to achieve the desired natural frequencies, the volume fractions of the constituents of the symmetric FG sandwich beam can be arranged. In order to verify the accuracy of the results obtained from the present method, a corresponding beam is also solved by ANSYS®. In Figure 3, it seems to be in excellent agreement with both results of ANSYS® and the present analytical solutions for the case considered in this study.

4.2 Effect of geometric index

Figure 4 depicts the variations of the natural frequencies of an FG beam with n=1 and k_s=100 versus geometric index (β) for C-F boundary conditions. It can be seen from Figure 4 that natural frequencies gradually decrease with changing from narrowing to expanding of the cross section for the C-F beam. As a result, narrowing beams can provide more advantages than expanding beams because less material is used, and they have higher natural frequencies than expanding beams. It is also seen that the results of the present and ANSYS® solutions are very close to each other.

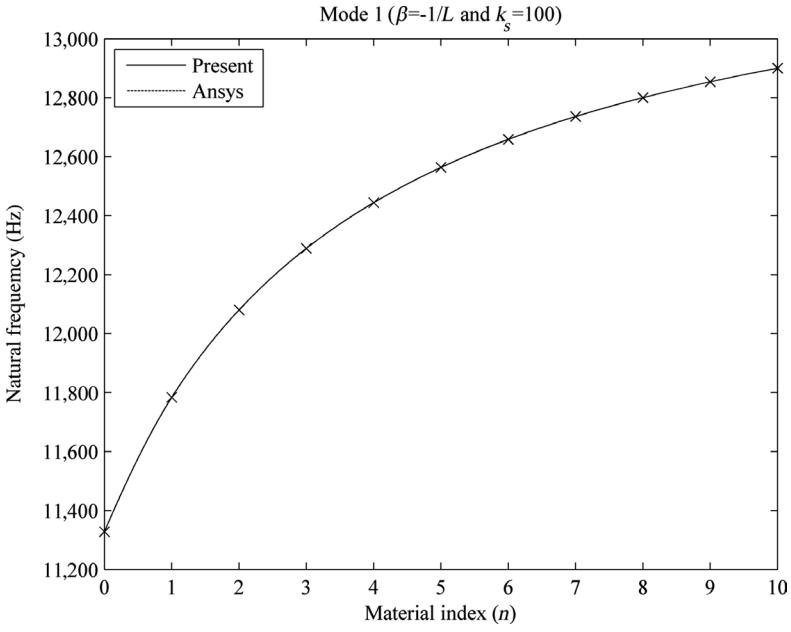

Figure 3 Variations of the natural frequencies with material index (n) for C-F boundary conditions (β=-1/L, k_s=100).

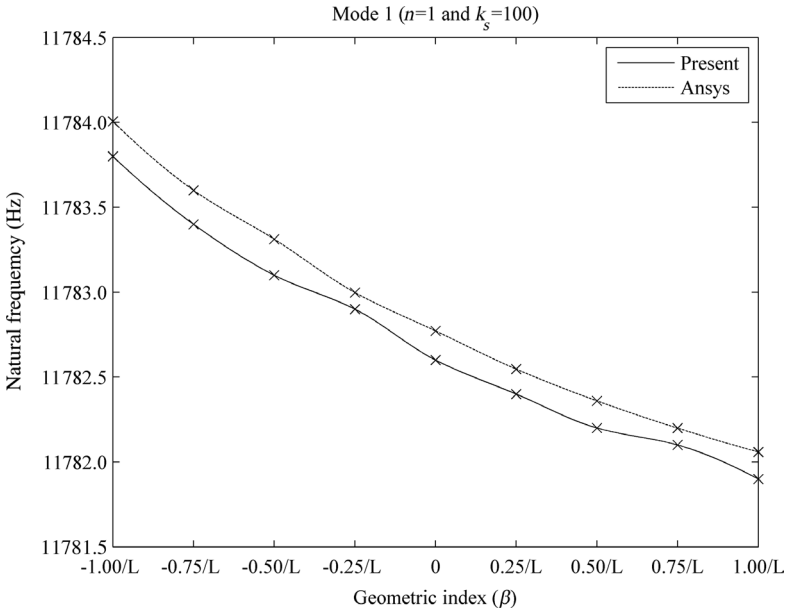

Figure 4 Variations of the natural frequencies with geometric index (β) for C-F boundary conditions (n=1 and k_s=100).

4.3 Effect of elastic foundation index

Figure 5 shows the variations of the natural frequencies of an FG beam with β=-1/L and n=1 versus elastic foundation index (k_s) for C-F boundary conditions. It can be seen that natural frequencies increase with increasing elastic foundation index (k_s). It is also seen that the increase in natural frequencies is relatively apparent when $k_s \leq 100$, whereas it becomes considerably slow when $k_s > 100$. From Figure 5, it is shown that the results of the present analytical solutions have an excellent agreement with the results of ANSYS® solutions for C-F boundary conditions.

4.4 Effect of the combining of all indexes

The first three natural frequencies of the symmetric FG sandwich beam on variable Winkler elastic foundation under three different types of boundary conditions are

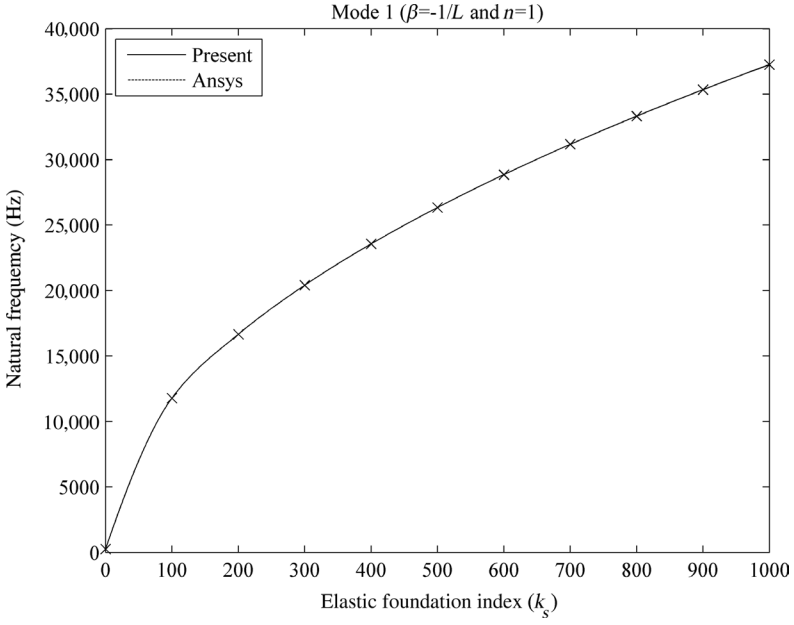

Figure 5 Variations of the natural frequencies with elastic foundation index (k_s) for C-F boundary conditions (β=-1/L and n=1).

Table 3 First three natural frequencies (Hz) of the sandwich beam on elastic foundation.

k_s	β=-1/L			β=0			β=1/L		
	n=0	n=1	n=10	n=0	n=1	n=10	n=0	n=1	n=10
Simply supported-simply supported									
0	550.5	513.6	401.1	555.9	518.6	405.1	550.5	513.6	401.1
	2229.0	2079.4	1624.2	2223.8	2074.6	1620.4	2229.0	2079.4	1624.2
	5011.6	4675.4	3651.9	5003.5	4667.8	3646.0	5011.6	4675.4	3651.9
10^2	11338.3	11792.4	12905.0	11338.6	11792.6	12905.1	11338.3	11792.4	12905.0
	11542.2	11963.3	13000.6	11541.2	11962.4	13000.1	11542.2	11963.3	13000.6
	12384.3	12675.0	13405.8	12381.0	12672.2	13404.1	12384.3	12675.0	13405.8
10^3	35816.9	37258.9	40791.4	35817.0	37259.0	40791.5	35816.9	37258.9	40791.4
	35882.0	37313.3	40821.8	35881.6	37313.1	40821.6	35882.0	37313.3	40821.8
	36161.6	37547.6	40952.6	36160.5	37546.6	40952.1	36161.6	37547.6	40952.6
Clamped-clamped									
0	1268.1	1183.0	924.0	1260.3	1175.7	918.3	1268.1	1183.0	924.0
	3484.5	3250.7	2539.1	3474.0	3240.9	2531.4	3484.5	3250.7	2539.1
	6821.9	6364.2	4971.0	6810.4	6353.4	4962.6	6821.9	6364.2	4971.0
10^2	11395.7	11840.4	12931.8	11394.9	11839.7	12931.4	11395.7	11840.4	12931.8
	11848.9	12221.4	13146.3	11845.8	12218.8	13144.8	11848.9	12221.4	13146.3
	13220.9	13390.3	13823.5	13215.0	13385.1	13820.5	13220.9	13390.3	13823.5
10^3	35835.1	37274.1	40799.9	35834.8	37273.9	40799.8	35835.1	37274.1	40799.9
	35981.8	37396.9	40868.4	35980.8	37396.1	40867.9	35981.8	37396.9	40868.4
	36456.6	37795.0	41091.2	36454.5	37793.2	41090.2	36456.6	37795.0	41091.2
Clamped-simply supported									
0	930.1	867.7	677.7	868.5	810.2	632.9	809.9	755.6	590.2
	2878.6	2685.4	2097.6	2814.5	2625.6	2050.9	2766.1	2580.5	2015.6
	5938.3	5539.9	4327.1	5872.2	5478.2	4278.9	5825.7	5434.8	4245.1
10^2	11363.1	11813.1	12916.5	11358.2	11809.0	12914.3	11353.9	11805.4	12912.3
	11685.1	12083.4	13068.2	11669.4	12070.2	13060.8	11657.9	12060.5	13055.3
	12787.4	13018.7	13605.2	12756.8	12992.6	13590.0	12735.5	12974.3	13579.3
10^3	35824.7	37265.5	40795.1	35823.2	37264.2	40794.4	35821.8	37263.0	40793.7
	35928.2	37352.0	40843.3	35923.1	37347.8	40841.0	35919.3	37344.6	40839.2
	36301.7	37665.0	41018.3	36290.9	37656.0	41013.3	36283.4	37649.7	41009.8

listed in Table 3. The effect of geometric, material and elastic foundation indexes are taken into account in this table. It can be seen from Table 3 that for the beam with symmetrical boundary conditions, i.e., S-S and C-C, the natural frequencies are symmetrical according to the beam of uniform cross section by increasing β, but they decrease with increasing n for k_s=0. As for k_s>0, they increase with increasing n. It can also be seen from Table 3 that for the beam with nonsymmetrical boundary conditions, i.e., C-S, the natural frequencies decrease with increasing β for all k_s values, whereas they decrease with increasing n for k_s=0 and increase with increasing n for k_s>0.

4.5 Effect of the slenderness ratio

The variations of the natural frequencies against the slenderness ratio (L/h) for material index n=1, elastic foundation index k_s=100 and geometric index β=-1/L are depicted in Figure 6. As expected, natural frequencies decrease with increasing slenderness ratio. Especially, whereas the natural frequencies of the beam reduce sharply for slenderness ratio between 5 and 10, they decline slowly after L/h=10.

4.6 Mode shapes

In Figures 7 and 8, the first mode shape of the cantilever FG beam with β=-1/L is derived for various material indexes n and elastic foundation indexes k_s, respectively. It can be seen that the mode shapes of the FG beams with different material indexes and elastic foundation indexes are very close to each other. Namely, the influences of the material index and elastic foundation index on the mode shape of the beam are quite limited.

The first displacement of the cantilever FG beam with n=1 and k_s=100 is shown in Figure 9 for different geometric indexes. The geometric index has an insignificant effect

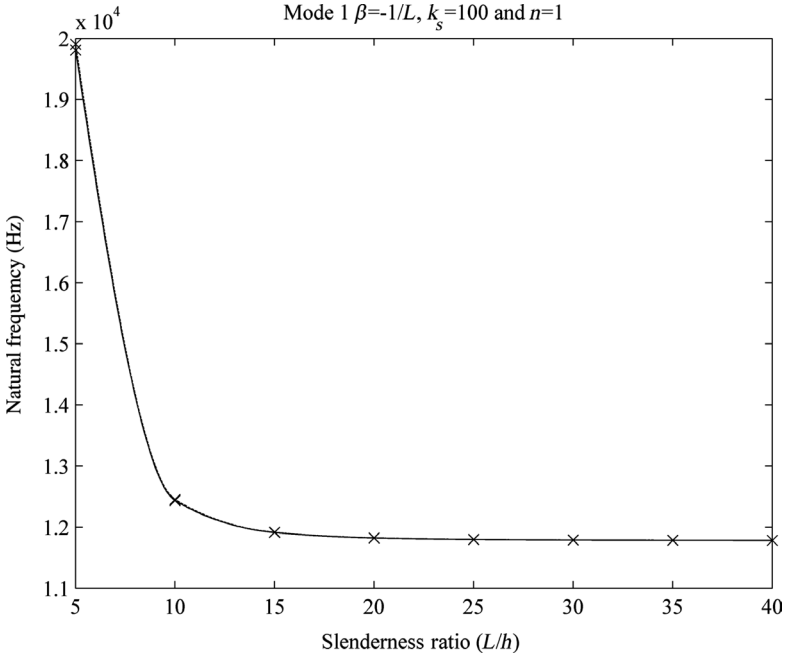

Figure 6 Variations of the natural frequencies with slenderness ratio (L/h) for C-F boundary conditions (β=-1/L, k_s=100 and n=1).

on the mode shape for cantilever FG beam. It is found that the maximum amplitude occurs at the right end of the narrowing cantilever beam. It is also seen from Figure 9 that the amplitude of the beam decreases with expanding width at the right end of the beam.

Figure 10 demonstrates the change in the fundamental vibration mode shape of FG beams for different length-to-height ratios as β=-1/L, k_s=100 and n=1. It can be seen in Figure 10 that slenderness ratio has no effect on the amplitude at the right end of the beam.

Finally, the first four bending eigenmodes are shown in Figure 11. It can be seen that the absolute value of amplitudes for all modes are almost the same at the right end of the beam. Nevertheless, the first and the third mode curves take place at completely opposite directions according to the second and the fourth mode.

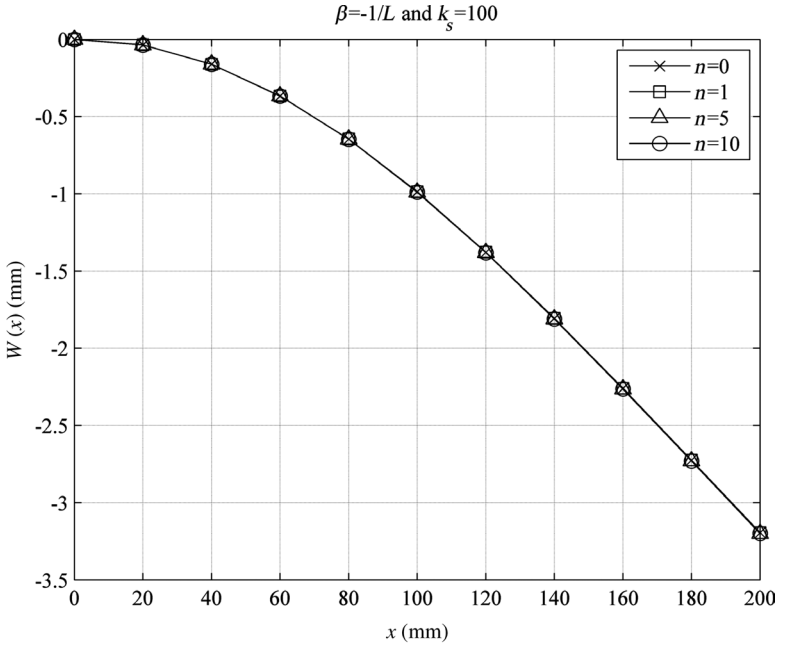

Figure 7 The first mode shape of the cantilever FG beam on elastic foundation for various material indexes (β=-1/L, k_s=100).

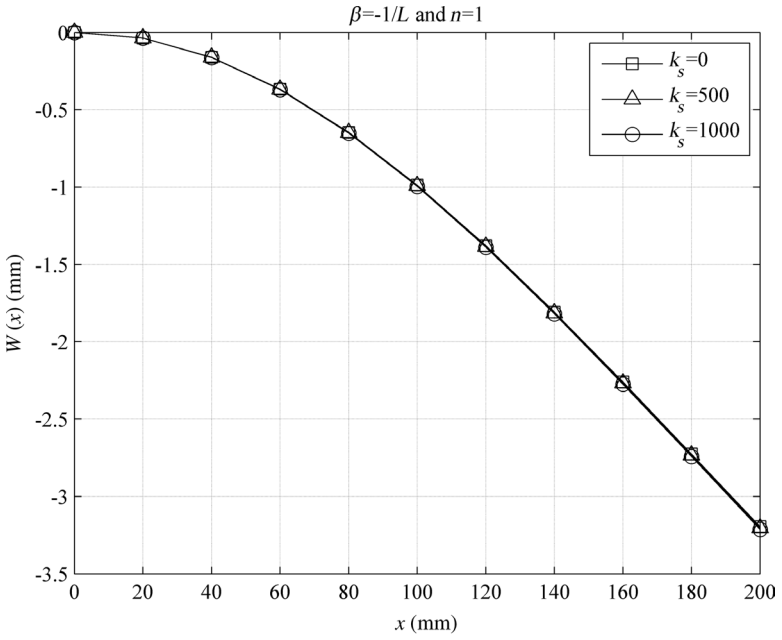

Figure 8 The first mode shape of the cantilever FG beam for various elastic foundation indexes (β=-1/L and n=1).

5 Conclusion

The free vibration of a symmetric FG sandwich beam with variable cross section resting on variable Winkler elastic foundation is investigated in this paper, and the verification is carried out by the results obtained from ANSYS® commercial software. Effects of material index, geometric index, elastic foundation index and slenderness ratio on vibration behavior of the FG beams are investigated. The following conclusions can be drawn from the analyses:

– The effective elasticity modulus and the effective mass density can be used instead of elasticity modulus and

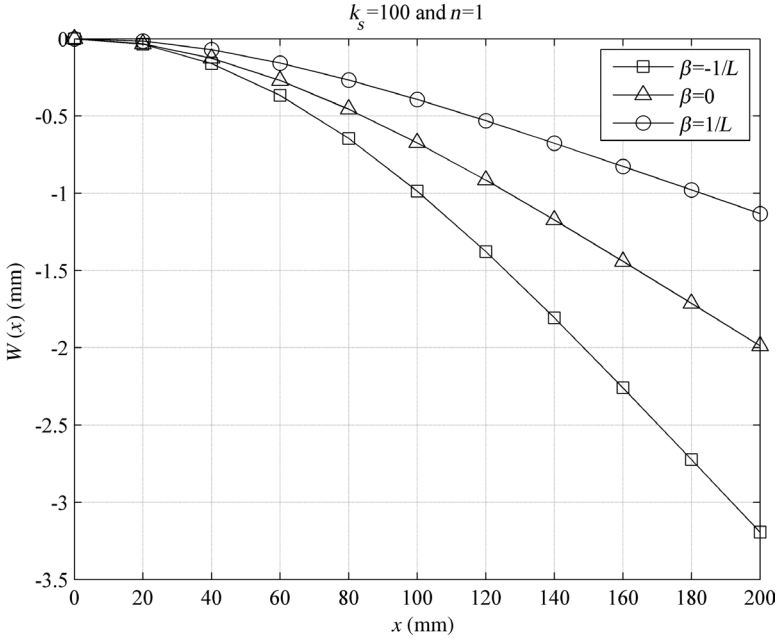

Figure 9 The first mode shape of the cantilever FG beam on elastic foundation for various geometric indexes (k_s=100 and n=1).

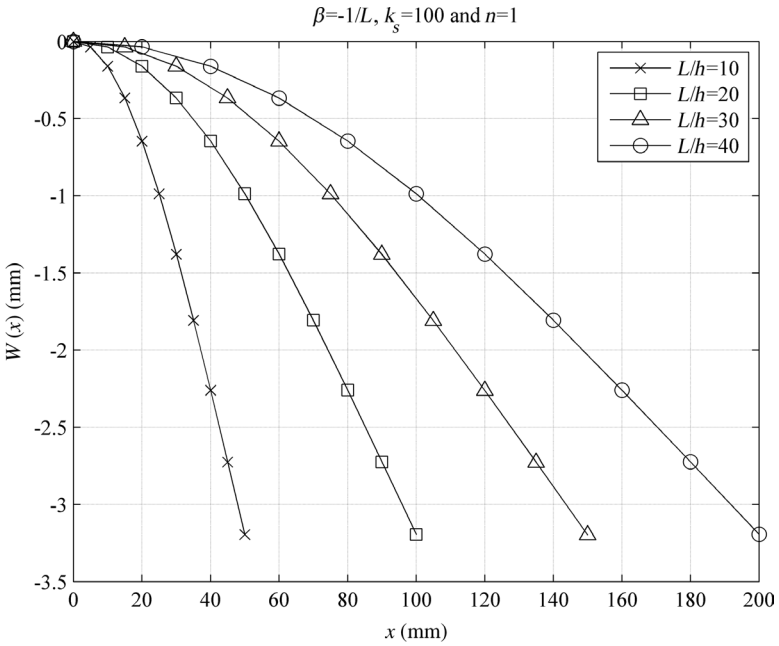

Figure 10 The first mode shape of the cantilever FG beam on elastic foundation for various slenderness ratios (β=-1/L, k_s=100 and n=1).

mass density in the governing differential equation of motion for a beam made of conventional materials.

- Increase in the volume fractions of the ceramic in the symmetric FG sandwich beam causes decrease in the natural frequencies.
- The natural frequencies decrease gradually with increasing geometric index.
- The natural frequencies increase with increasing elastic foundation index (k_s). The increase in natural frequencies is relatively apparent when $k_s \leq 100$, whereas it becomes considerably slow when $k_s > 100$.
- The natural frequencies of the beam reduce sharply for slenderness ratio between 5 and 10, whereas they decline slowly after L/h=10.

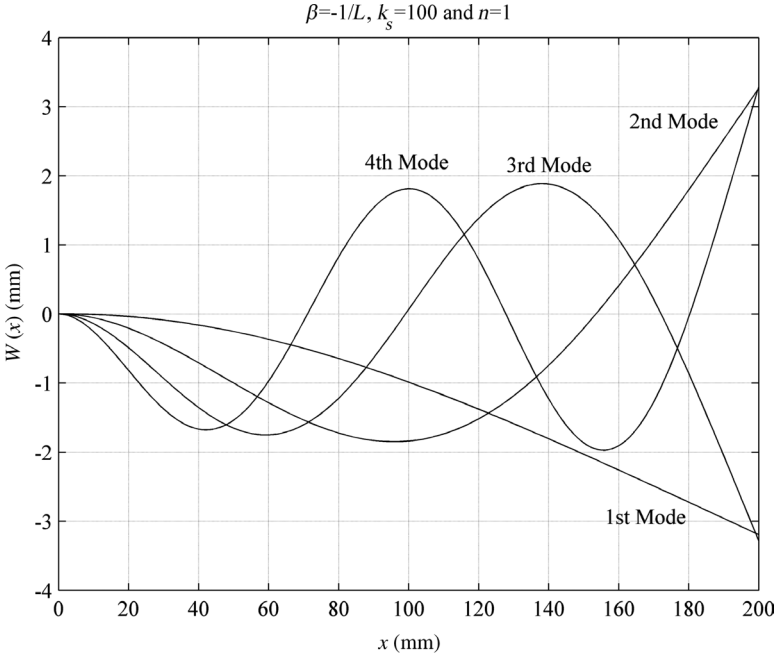

Figure 11 The first four mode shape of the cantilever FG beam on elastic foundation (β=-1/L, k_s=100 and n=1).

- The effects of the material index and elastic foundation index on the mode shape of the beam are quite limited.
- The amplitude at the right end of the beam decreases with expanding width at the right end of the beam.
- The slenderness ratio has no effect on the amplitude at the right end of the beam.

Acknowledgements: The authors would like to thank the Pamukkale University Scientific Research Council for supporting this study under Project Contract No. 2011BSP014.

Received November 23, 2012; accepted March 18, 2013; previously published online April 11, 2013

References

[1] Çallioğlu H, Sayer M, Demir E. *Indian J. Eng. Mater. Sci.* 2011, 18, 111–118.
[2] Sankar BV. *Compos. Sci. Technol.* 2001, 61, 689–696.
[3] Zhong Z, Yu T. *Compos. Sci. Technol.* 2007, 67, 481–488.
[4] Benatta MA, Mechab I, Tounsi A, Bedia EAA. *Comput. Mater. Sci.* 2008, 44, 765–773.
[5] Aydogdu M, Taskin V. *Mater. Des.* 2007, 28, 1651–1656.
[6] Aydogdu M. *J. Reinf. Plast. Compos.* 2008, 27, 683–691.
[7] Pradhan SC, Murmu T. *J. Sound Vib.* 2009, 321, 342–362.
[8] Bedjilili Y, Tounsi A, Berrabah HM, Mechab I, Bedia EAA, Benaissa S. *J. Appl. Math. Mech. (Engl. Transl.)* 2009, 30, 717–726.
[9] Murín J, Aminbaghai M, Kutis V. *Eng. Struct.* 2010, 32, 1631–1640.
[10] Mahi A, Bedia EAA, Tounsi A, Mechab I. *Compos. Struct.* 2010, 92, 1877–1887.
[11] Ece MC, Aydogdu M, Taskin V. *Mech. Res. Commun.* 2007, 34, 78–84.
[12] Atmane HA, Tounsi A, Meftah SA, Belhadj HA. *J. Vib. Control* 2011, 17, 311–318.
[13] Cranch ET, Adler AA. *ASME J. Appl. Mech.* 1956, 23, 103–108.
[14] Caruntu D. *Solid Mech. Its Appl.* 1999, 73, 109–118.
[15] Datta AK, Sil SN. *Comput. Struct.* 1996, 59, 479–483.
[16] Laura PAA, Gutierrez RH, Rossi RE. *Ocean Eng.* 1996, 23, 1–6.
[17] Ayvaz Y, Özgan K. *J. Sound Vib.* 2002, 255, 111–127.
[18] Motaghian SE, Mofid M, Alanjari P. *Sci. Iran.* 2011, 18, 861–866.
[19] Ying J, Lue CF, Chen WQ. *Compos. Struct.* 2008, 84, 209–219.
[20] Gibson RF. *Principles of Composite Material Mechanics*, McGraw-Hill: Singapore, 1994.